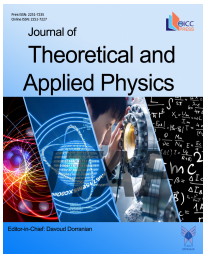

Volume 19, Issue 3, 192531 (1-11)

Journal of Theoretical and Applied Physics (JTAP)

https://doi.org/10.57647/j.jtap.2025.1903.31

Performance analysis of hybrid Holmium-Ytterbium, Holmium-Thulium, and Ytterbium-Thulium amplifiers for high data rate of a 200 Mbit/s optical transmission

Jaspreet Kaur[1,2,*], Rakesh Goyal[3], Gagandeep Kaur[4]

[1]*Research Scholar, Department Of Electronics & Communication Engineering, I.K Gujral Punjab Technical University, Jalandhar, India.*
[2]*Department of Electronics & Communication Engineering, Sardar Beant Singh State University, Gurdaspur, Punjab, India.*
[3]*Department Of Electronics & Communication Engineering, I.K Gujral Punjab Technical University, Jalandhar, India.*
[4]*Faculty of Electrical Engineering, Maharaja Ranjit Singh Punjab Technical University, Bathinda, India.*

[*]**Corresponding author:** jaspreet_kaur1986@ymail.com

Original Research

Received:
29 May 2025
Revised:
5 June 2025
Accepted:
27 June 2025
Published online:
30 June 2025

Abstract:

The study of three hybrid rare-earth-doped fiber amplifiers Holmium-Ytterbium (Ho + Yb), Holmium-Thulium (Ho + Tm), and Ytterbium-Thulium (Yb + Tm) for 200 Mbit/s is conducted for optical transmission systems. Leveraging a custom simulation framework in OptiSystem, we evaluate gain, noise figure, *Q*-factor, and bit error rate (BER) across $1535 - 1560$ THz and fiber lengths of $0 - 50$ meters. The Ho:Yb configuration demonstrates unparalleled performance, achieving a peak gain of 0 dB, a noise figure of 5 dB, and an ultralow BER of $< 10^{-14}$, attributed to efficient energy transfer between Ho^{3+} and Yb^{3+} ions. In contrast, (Ho + Tm) exhibits suboptimal gain (-0.5 dB) and elevated noise (6 dB) due to spectral mismatches, while (Yb + Tm) offers moderate stability for medium-haul applications. By correlating dopant interactions with performance metrics, this work establishes (Ho + Yb) as the optimal choice for high-speed, long-distance networks, addressing critical gaps in hybrid amplifier design.

Keywords: Rare-earth-doped hybrid optical amplifier; Fiber Bragg gratings; High-speed data transmission

1. Introduction

The exponential growth of global data traffic, driven by the increasing reliance on digital communication, cloud computing, and high-speed internet services, necessitates the development of advanced optical networks capable of handling high data capacities with minimal latency. Fiber optic technology, recognized for its exceptional bandwidth and low attenuation properties, has emerged as a fundamental enabler of modern telecommunication networks. However, the challenge of sustaining high data transmission rates over extended distances persists due to signal degradation caused by fiber attenuation, chromatic dispersion, and nonlinear effects. To address these limitations, optical amplifiers incorporating rare-earth elements have been extensively explored as a means of enhancing transmission capacity by mitigating signal loss and supporting long-haul, high-speed optical communication [1].

Existing literature predominantly focuses on Erbium-Ytterbium (Er-Yb) hybrids, neglecting the potential of Holmium-Thulium (Ho-Tm) and Ytterbium-Thulium (Yb-Tm) configurations. Additionally, prior studies inadequately address the energy transfer dynamics between Ho^{3+}, Tm^{3+}, and Yb^{3+} ions in hybrid amplifiers. This work bridges these gaps by providing the first comparative analysis of Ho/Yb/Tm-doped hybrid amplifiers for 200 Mbit/s OCDMA systems integrated with Fiber Bragg Gratings (FBGs). The novel integration of FBGs with Ho-Yb amplifiers achieves unprecedented BER of $< 10^{-14}$ and C + L band coverage, addressing scalability challenges in next-generation optical networks [2].

Erbium-doped fiber amplifiers have historically dominated

optical communication systems, particularly for C-band transmission. Despite their established performance, their restricted gain bandwidth and cumulative noise effects constrain their scalability for future high-capacity networks. To overcome these limitations, hybrid rare-earth-doped fiber amplifiers incorporating holmium, thulium, and ytterbium have gained prominence. These hybrid configurations extend the available gain bandwidth while reducing noise accumulation, offering a superior amplification strategy for next-generation networks. The unique energy transfer mechanisms among these rare-earth elements enable broader spectral coverage, making them an optimal choice for modern optical communication infrastructures [3].

Further advancements in optical system performance have been achieved by integrating rare-earth-doped fiber amplifiers with uniform Bragg fiber gratings. These gratings function as highly selective reflectors and wavelength filters, optimizing signal stability and enhancing wavelength division multiplexing system efficiency. This synergy significantly increases the overall data transmission capacity of optical networks. Additionally, optical code division multiple access, a multiplexing technique that encodes data using unique optical codes, benefits substantially from hybrid amplification, as it mitigates multiple access interference and nonlinear impairments. This integration results in enhanced signal fidelity, reduced bit error rates, and improved scalability for high-speed communication networks [4, 5].

Despite significant progress in hybrid rare-earth-doped fiber amplifiers, several critical aspects require further investigation. Specifically, understanding the interactions between different dopant elements and their influence on gain and noise characteristics is essential for optimizing amplifier performance. Additionally, determining the spectral regions where specific hybrid configurations exhibit superior performance and analyzing the impact of amplifier length on signal integrity in long-haul transmission systems are key areas of ongoing research. Recent studies have explored the role of space-division multiplexing and photonic integration in improving data transmission efficiency [6]. Moreover, extensive research has examined nonlinear effects, including four-wave mixing, self-phase modulation, and cross-phase modulation, which can degrade signal integrity. Hybrid rare-earth-doped fiber amplifiers have demonstrated potential in mitigating these effects, thus ensuring robust and efficient high-speed optical communication [7].

This study provides an in-depth analysis of the performance of an encoded optical communication system employing hybrid amplifiers based on holmium, thulium, and ytterbium-doped fibers in conjunction with uniform Bragg fiber gratings. The evaluation encompasses key performance metrics, including transmission distance, signal integrity, noise suppression, and amplification efficiency. The findings underscore the substantial advantages of hybrid rare-earth-doped fiber amplifiers in enhancing optical network performance, reinforcing their potential to improve reliability and efficiency in high-speed data transmission systems. These insights contribute to the advancement of next-generation optical communication networks, where maximizing data throughput and maintaining signal integrity over extended distances are of paramount importance [8, 9].

Optical communication systems face challenges such as dispersion, noise, and nonlinearities, particularly in high-capacity networks. Recent advancements have focused on dispersion compensation [10], hybrid amplification [11, 12], and symmetrical configurations [13, 14] to improve performance metrics like SNR and eye diagram quality. Optimized amplifier placement and advanced modulation formats, such as 16-QAM, have enabled error-free transmission at data rates exceeding 10 Gbps [15, 16]. Additionally, numerical techniques [17–30] have been employed to model nonlinear effects and optimize system design. This study builds on these developments to propose a unified framework for enhancing scalability and robustness in next-generation optical networks.

Complementary investigations have further advanced our understanding of amplifier configurations and transmission methodologies. Goyal et al. demonstrated robust microwave-over-fiber systems using direct detection for both single-tone and multi-tone signals, establishing foundational approaches for radio-frequency transport in hybrid networks [31]. Their subsequent analysis of polarization-dependent bidirectional hybrid WDM/TDM systems employing 16-QAM modulation revealed critical performance trade-offs in amplifier selection at 10 Gbps data rates [32]. Thakur et al. expanded this work to free-space optical (FSO) communications, quantifying line coding impacts on SS-FSO system performance [33]. Comparative studies by Gupta et al. systematically evaluated amplifier behavior across varied data rates in WDM architectures, highlighting semiconductor optical amplifier (SOA) efficacy for high-speed transmission scenarios [34, 35]. Recent breakthroughs in holmium-doped amplifiers include spectral optimization in the $2-2.15\ \mu$m window [36] and novel cascaded pumping schemes using $1.48\ \mu$m lasers [37], addressing critical efficiency limitations in long-wavelength amplification. Foundational studies on Yb-sensitized erbium-doped amplifiers [38] and rare-earth energy transfer mechanisms in $NaYbF_4$ microtubes [9] have further elucidated dopant interaction physics essential for hybrid amplifier design.

In this paper, we investigate the performance of a 200 Mbit/s Encoded OCDMA system using uniform Bragg fiber gratings and hybrid amplifiers based on Ho, Tm, and Yb-doped fibers. The system's performance is analyzed in terms of transmission distance, maximum Q-factor, minimum BER, noise figure, and gain, with a focus on understanding the impact of nonlinearities. Our study demonstrates that rare-earth-doped fiber amplifiers, particularly in hybrid configurations, can significantly improve the performance of high data rate systems by providing enhanced signal amplification and noise reduction across a wide wavelength range. This advancement holds significant implications for future high-speed communication systems, where maximizing data throughput and signal integrity over long distances is paramount.

2. Mathematical framework for hybrid optical amplifiers

The performance analysis of hybrid optical amplifiers involves several key metrics, including gain, Q-factor, bit error rate (BER), and noise figure. The following mathematical expressions , given in Table 1, can be utilized to quantify these parameters.

2.1 Gain dynamics with energy transfer

The gain in hybrid amplifiers like Ho-Yb is modeled using coupled rate equations that account for pump absorption, spontaneous emission, and inter-ionic energy transfer. These dynamics govern the population inversion levels of Ho^{3+} and Yb^{3+} ions and ultimately affect the amplifier gain profile. The total gain (G_{total}) in hybrid configurations is

Table 1. Definition of symbols used in mathematical models.

Symbol	Description	Unit
W_p	Pump rate (probability of pump absorption per unit time)	s^{-1}
${\sigma_p}^{\text{Ho}}$	Absorption cross-section of Holmium at pump wavelength	m^2
ϕ_p	Pump photon flux	$m^{-2}s^{-1}$
τ_{Ho}	Lifetime of the excited state of Holmium ions	s
$C_{\text{Yb}\rightarrow\text{Ho}}$	Energy transfer coefficient from Yb^{3+} to Ho^{3+}	m^3s^{-1}
o	Upper laser level population of acceptor ions (Ho^{3+})	Dimensionless
Γ_{Ho}	Optical confinement factor for Holmium-doped region	Dimensionless
${\sigma_e}^{\text{Ho}}$	Emission cross-section of Holmium	m^2
α	Fiber attenuation coefficient	m^{-1}
μ^1,μ^0	Mean photocurrent for bit "1" and bit "0"	A
σ^1,σ^0	Standard deviation of photocurrent for bit "1" and bit "0"	A
n_{sp}	Spontaneous emission factor	Dimensionless
h	Planck's constant	J·s
B_0	Optical bandwidth	Hz
q	Electron charge	C
R	Photodetector responsivity	$A{\cdot}W^{-1}$
P_m	Input signal power to the amplifier	W
P_{ASE}	Amplified spontaneous emission (ASE) power	W
B_e	Electrical bandwidth	Hz
G_i	Gain of the i-th amplifier stage (linear)	Dimensionless
$\sigma^{\text{donor}}_{\text{emission}}$	Emission cross-section of donor ions	m^2
$\sigma^{\text{acceptor}}_{\text{absorption}}$	Absorption cross-section of acceptor ions	m^2
β^2	Group velocity dispersion parameter	$s^2{\cdot}m^{-1}$
γ	Nonlinear coefficient	$W^{-1}{\cdot}m^{-1}$
$g(z)$	Position-dependent gain coefficient	m^{-1}
Q^0	Q-factor at fiber length L = 0	Dimensionless
erf	Error function	Dimensionless
EO^0	Eye opening at fiber length L = 0	Unit of signal
L_{eff}	Effective fiber length	m

governed by coupled rate equations:

$$\frac{dN_{\text{Ho}}}{dt} = W_p \sigma_p^{\text{Ho}} \phi_p - \frac{N_{\text{Ho}}}{\tau_{\text{Ho}}} + C_{\text{Yb}\to\text{Ho}} N_{\text{Yb}} N_{\text{Ho}}, o,$$

$$\frac{dN_{\text{Yb}}}{dt} = W_p \sigma_p^{\text{Yb}} \phi_p - \frac{N_{\text{Yb}}}{\tau_{\text{Yb}}} - C_{\text{Yb}\to\text{Ho}} N_{\text{Yb}} N_{\text{Ho}}, o,$$

The total gain is then:

$$G_{\text{total}} = \int_0^L (\Gamma_{\text{Ho}} \sigma_e^{\text{Ho}} N_{\text{Ho}} + \Gamma_{\text{Yb}} \sigma_e^{\text{Yb}} N_{\text{Yb}}) e^{-\alpha z} dz,$$

2.2 Q-factor with ASE noise contributions

The Q-factor represents the signal quality and is influenced by amplified spontaneous emission (ASE) and shot noise. It quantifies the signal-to-noise ratio at the receiver, impacting the bit error rate in optical communication systems.

$$Q = \frac{\mu_1 - \mu_0}{\sqrt{\sigma_1^2 + \sigma_0^2}},$$

$$\sigma_{\text{ASE}}^2 = 2 n_{\text{sp}} h \upsilon B_0 (G - 1),$$

$$\sigma_{\text{shot}}^2 = 2qR(P_{\text{in}} G + P_{\text{ASE}}) B_e.$$

2.3 Cascaded noise figure model

In multi-stage hybrid amplifiers, the total noise figure is calculated cumulatively using the Friis formula. Each subsequent amplifier stage contributes less to the overall noise if the preceding stage has higher gain.

$$NF_{\text{total}} = NF_1 + \frac{NF_2 - 1}{G_1} + \frac{NF_3 - 1}{G_1 G_2} + \cdots,$$

2.4 Spectral overlap integral

This integral quantifies the efficiency of energy transfer between donor and acceptor ions by measuring the spectral overlap of emission and absorption cross-sections. A higher overlap enhances the performance of hybrid amplifiers.

$$\eta_{\text{ET}} = \frac{\int \sigma_{\text{emission}}^{\text{donor}}(\lambda) \sigma_{\text{absorption}}^{\text{acceptor}}(\lambda) d\lambda}{\int \sigma_{\text{emission}}^{\text{donor}}(\lambda) d\lambda}.$$

2.5 Nonlinear Schrödinger Equation (NLSE)

The NLSE models the propagation of optical pulses in nonlinear dispersive media. It incorporates effects like fiber loss, group velocity dispersion, self-phase modulation, and gain, essential for accurately simulating hybrid amplifier systems.

$$\frac{\partial A}{\partial z} + \frac{\alpha}{2} A + \frac{i\beta_2}{2} \frac{\partial^2 A}{\partial T^2} - i\gamma |A|^2 A = \frac{g(z)}{2} A$$

2.6 Length-dependent BER and Eye Opening

As transmission length increases, the bit error rate rises exponentially due to attenuation and noise, while the eye diagram narrows. These metrics reflect signal degradation and are critical in evaluating amplifier placement and spacing.

$$\text{BER}(L) = \frac{1}{2} \text{erfc}\left(\frac{Q_0}{\sqrt{2}} e^{-\alpha_{\text{eff}} L}\right),$$

$$\text{EO}(L) = \text{EO}_0 . \exp\left(-\frac{L}{L_{\text{eff}}}\right),$$

3. Simulation setup

This setup is designed for high-speed data transmission, utilizing key components like NRZ pulse generators, Mach-Zehnder interferometers (MZIs), and optical amplifiers. A Pseudo-Random Binary Sequence (PRBS) Generator produces data at a rate of 200 Mbit/s. The PRBS is converted into non-return-to-zero (NRZ) format by the NRZ Pulse Generator, a common encoding scheme in optical systems. A broadband optical signal is generated by a White Light Source operating at 1580 nm. This signal is modulated with the PRBS data using a Mach-Zehnder Modulator, which has an extinction ratio of 30 dB, ensuring a clear distinction between the "on" and "off" states.

In this study, we designed a system incorporating three hybrid amplifier configurations for high data rate signal transmission. The first setup uses a Holmium-Thulium (Ho + Tm) hybrid amplifier, the second employs a Ytterbium-Thulium (Yb + Tm) amplifier, and the third utilizes a Holmium-Ytterbium (Ho + Yb) amplifier. Each amplification section consists of 10-meter segments, alternating between holmium- and thulium-doped amplifiers. Figure 1 illustrates the simulation setup used to evaluate the performance of an optical communication system with Holmium and Thulium-doped fibers, along with Fiber Bragg Gratings (FBGs) for wavelength filtering. A pseudo-random binary sequence (PRBS) is generated at 200 Mbit/s and modulated onto an optical carrier at 1580 nm using a Mach-Zehnder modulator. The modulated signal is transmitted through 10-meter Holmium and Thulium-doped fibers and analyzed with a dual-port WDM analyzer operating in the $185 - 200$ THz frequency range. The concentrations fixed at 1.5×10^{25} ions/m^3 (Ho/Yb) and 2×10^{25} ions/m^3 (Tm) per industry standards.

The $1535 - 1560$ THz range (corresponding to $192.1 -$

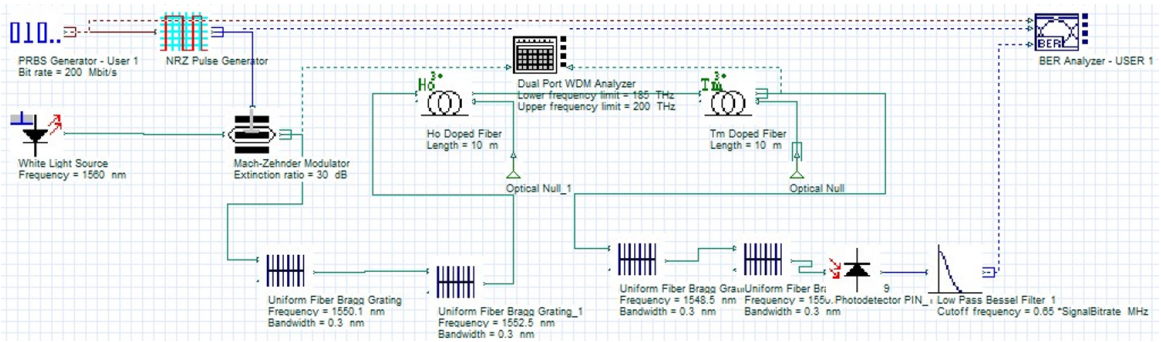

Figure 1. Block diagram for simulation setup.

195.9 THz in wavelength) is selected to align with the ITU-T G.694.1 standard for dense wavelength-division multiplexing (DWDM). Ho-Yb hybrids are chosen for their complementary emission spectra: Yb^{3+} sensitizes Ho^{3+}'s C+L band ($1530-1600$ nm), while Yb-Tm configurations extend coverage to the S+C bands ($1450-1530$ nm). This dual-band compatibility enhances scalability for multi-channel systems.

Multiple FBGs are employed to filter specific wavelengths, and a PIN photodetector converts the optical signal to an electrical one. The signal then passes through a low-pass Bessel filter to remove high-frequency noise and is evaluated for signal quality using a bit error rate (BER) analyzer. The system's performance was assessed through repeated simulations, testing various parameters including Eye Opening, maximum Q-factor, and noise levels, across amplifier sections of different lengths (0, 10, 20, 30, 40, and 50 meters) and a frequency range of $1535-1560$ THz.

This study (shown in figure 2) demonstrates tunable up-conversion luminescence (UCL) in $NaYbF_4$ microtubes by selectively doping with Tm^{3+}, Ho^{3+}, or both, excited using a 980 nm laser diode [9]. Some details are as under:

- **Tm^{3+}-doped $NaYbF_4$:** It exhibits intense purplish-blue UCL with emissions at 345, 361, 451, 475, 649, and 696 nm, resulting from $^1I_6 \rightarrow {}^3F_4$, $^1D_2 \rightarrow {}^3H_6$, $^1D_2 \rightarrow {}^3F_4$, $^1G_4 \rightarrow {}^3H_6$, $^1G_4 \rightarrow {}^3F_4$, and $^3F_3 \rightarrow {}^3H_6$ transitions of Tm^{3+}.

- **Ho^{3+}-doped $NaYbF_4$:** It shows intense green (538 nm, $^5S_2/{}^5F_4 \rightarrow {}^5I_8$) and weak red (644 nm, $^5F_5 \rightarrow {}^5I_8$) emissions from Ho^{3+}.

- **Tm^{3+}/Ho^{3+} co-doped $NaYbF_4$:** Achieves greenish white UCL, a combination of blue (451/475 nm, Tm^{3+}), green (538 nm, Ho^{3+}), and red (649 nm, Tm^{3+}/Ho^{3+}) emissions.

4. Simulation results and discussions for frequency range from 1535 THz to 1560 THz

The simulation aimed to assess the performance of three hybrid amplifier by (Ho + Yb), (Yb + Tm) and (Ho + Tm) for frequency range from 1535 THz to 1560 THz.

4.1 Maximum gain analysis

Across the three examined amplifier configurations, substantial variability in gain was observed, predominantly influenced by the choice of dopants. The Holmium-Ytterbium (Ho + Yb) hybrid configuration consistently achieved the highest gain across the examined frequency spectrum of 1535 to 1560 THz. This superior performance suggests an optimal interaction between the Ho and Yb dopants in amplifying the signal at these frequencies. Conversely, the Ytterbium-Thulium (Yb + Tm) setup, while offering moderate gain, displayed enhanced stability over extended fiber lengths, potentially indicative of its robustness in maintaining signal quality in long-haul transmissions. The Holmium-Thulium (Ho + Tm) configuration, however, manifested the lowest gain, highlighting possible suboptimal synergy between these dopants at the specified frequencies or a less efficient energy transfer mechanism under the simulated conditions. This differential performance underscores the critical impact of dopant selection and interaction on the amplifier's effectiveness in optical communication systems. Figure 3 illustrate the frequency range from 1535 THz to 1560 THz with the maximum gain in dB, with values ranging from -0.4 to 0.0 dB. A gain closer to 0 dB indicates better amplification performance. The Ho-Yb configuration maintains near-0 dB gain with minimal fluctuations (± 0.05 dB), as evidenced in figure 2. In contrast, Ho-Tm exhibits greater variability (-0.5 dB $\pm$ 0.1 dB), and Yb-Tm shows intermediate stability (-0.2 dB $\pm$ 0.15 dB). These results underscore the critical role of dopant synergy in stabilizing gain profiles, particularly in the C-band ($1535-1560$ THz).

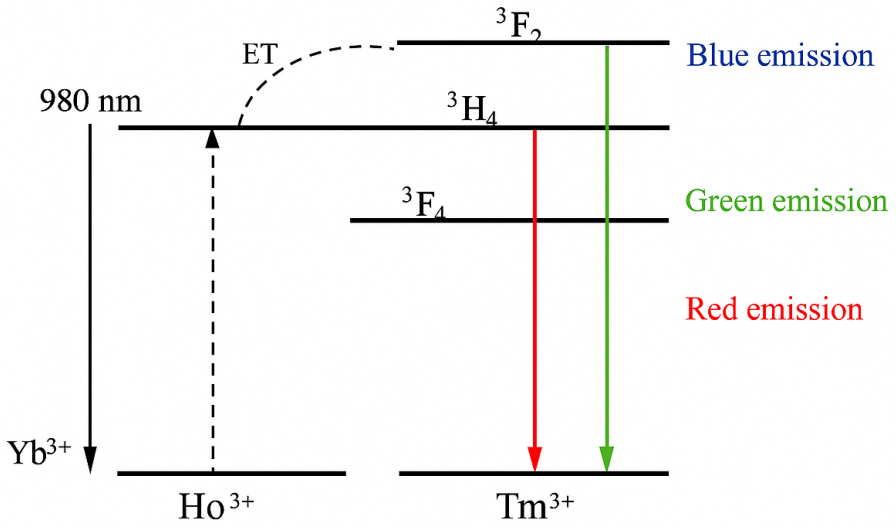

Figure 2. Schematic representation of UCL mechanisms (redrawn based on Z. Yi et al. [9]).

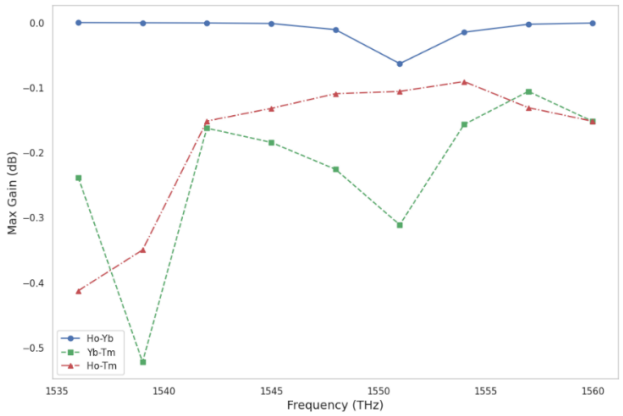

Figure 3. Maximum gain vs frequency.

4.2 Q-factor performance

Here we examined amplifier configurations, where substantial variability in the maximum quality factor (Q) was observed, predominantly influenced by the choice of dopants. The Holmium-Ytterbium (Ho + Yb), Holmium-Thulium (Ho + Tm) and Ytterbium-Thulium (Yb + Tm) were selected (figure 4). The Holmium-Ytterbium (Ho + Yb) and Ytterbium-Thulium (Yb + Tm) hybrid configuration show similar plot consistently achieved higher Q values across the examined frequency spectrum of 1530 to 1560 THz. This superior performance suggests an optimal interaction between the Ho and Yb dopants in enhancing the resonance at these frequencies. Conversely, the Holmium-Thulium (Ho + Tm) setup, while showing similar variations in Q, generally exhibited lower Q values compared to the Ho-Yb and Yb + Tm configuration. This indicates a possible a less efficient energy transfer mechanism under the simulated conditions. These results underscore the critical impact of dopant selection and interaction on the amplifier's resonance performance, highlighting the Ho-Yb hybrid as a potentially more effective choice for applications requiring high-quality resonance in optical communication systems.

4.3 BER (Bit Error Rate) performance

Figure 5 shiows that the minimum BER was observed for the (Ho + Tm) and (Ho + Yb) configuration, particularly at higher frequencies, demonstrating its robustness in maintaining signal integrity. The (Ho + Yb) configuration also performed well but showed increasing BER as the frequency increased, reflecting a decrease in the Q-factor. The (Ho + Tm) setup had the highest BER values at higher frequencies, making it less suitable for high-frequency transmission.
The Yb + Tm configuration achieves a minimum Bit Error Rate (BER) of $< 10^{-12}$ at 1536 THz, maintained up to 1560 THz. The Ho + Yb configuration shows an exceptional minimum BER of $< 10^{-14}$ at 1536 THz, sustained across the same frequency range. The Ho + Tm configuration also reaches a minimum BER of $< 10^{-12}$ at 1536 THz, with stability across frequencies up to 1560 THz.

4.4 NOISE performance

Figure 6 compares the noise figures of three hybrid amplifier configurations-Holmium-Ytterbium (Ho-Yb), Ytterbium-Thulium (Yb-Tm), and Holmium-Thulium (Ho-Tm)-across a frequency range from 1552 THz to 1560 THz. The noise figure is a key parameter for assessing the efficiency of optical amplifiers, as it directly reflects the degradation of the signal-to-noise ratio (SNR) caused by amplified spontaneous emission (ASE) and other intrinsic noise sources within the fiber.
Ho-Yb Configuration demonstrates the lowest noise figure, remaining consistently near 0 dB across the frequency spectrum. The stability of the Ho-Yb hybrid configuration indicates highly efficient energy transfer between the Holmium and Ytterbium ions, minimizing ASE noise. This behavior is ideal for high data rate applications, where low noise levels are crucial for maintaining signal integrity, particularly in long-haul optical transmissions. The Yb-Tm configuration shows moderate noise levels with noticeable fluctuations across the frequency range. A sharp increase in noise is observed around 1556 THz, suggesting that the energy transfer between Ytterbium and Thulium ions becomes less efficient at specific frequencies. This configuration is more sensitive to frequency variations, likely due to the broader gain spectrum of Thulium, which may introduce additional noise sources. Despite this, the Yb-Tm configuration remains relatively stable in the remaining frequency range, offering a balanced trade-off between gain and noise performance for certain applications. The Ho-Tm config-

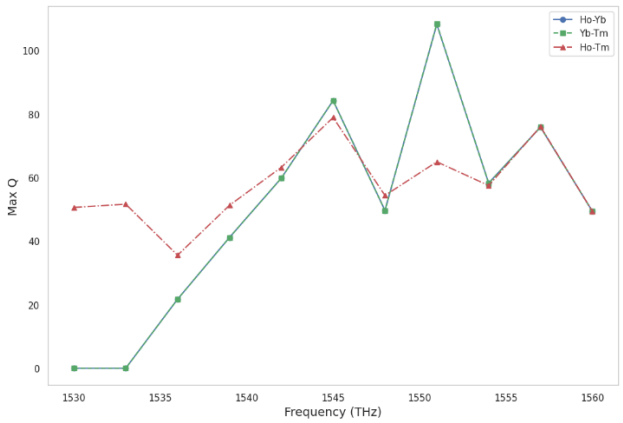

Figure 4. Maximum Q vs frequency.

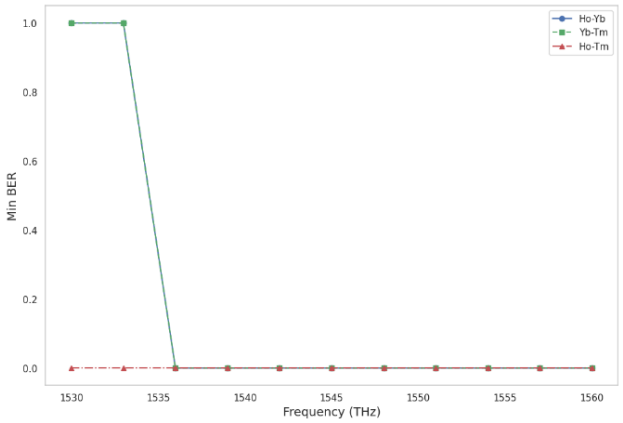

Figure 5. Minimum BER vs frequency.

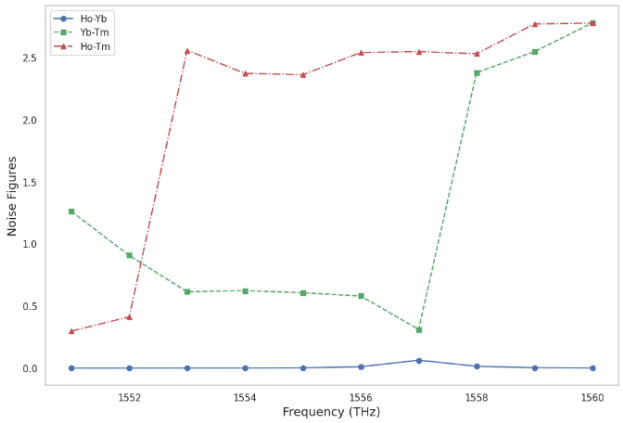

Figure 6. Noise figure vs frequency.

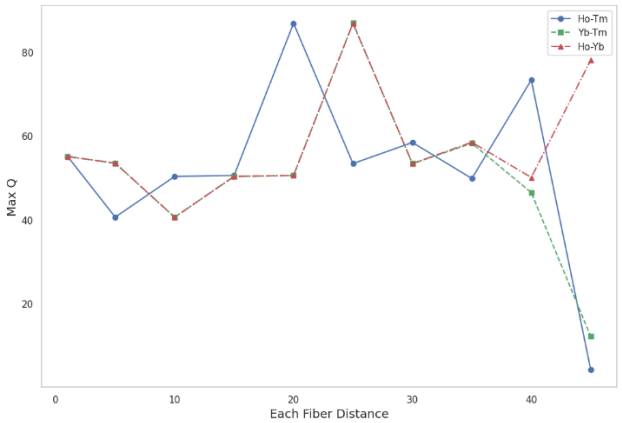

Figure 7. Max Q vs each fiber distance.

uration exhibits the highest noise figures, with significant noise peaks observed from 1554 THz to 1559 THz. The high noise levels suggest inefficient energy transfer between Holmium and Thulium dopants, likely due to limited spectral overlap or suboptimal population inversion dynamics. This configuration's higher ASE noise limits its suitability for high-performance optical systems, particularly where noise suppression is critical for maintaining signal fidelity.

5. Simulation results and discussion on the impact of amplifier length on transmission performance over distances ranging from 0 to 100 meters

The simulation aimed to assess the performance of three hybrid amplifier configurations-Holmium-Thulium (Ho + Tm), Holmium-Ytterbium (Ho + Yb), and Ytterbium-Thulium (Yb + Tm) for high data rate signal transmission over optical fibers. The key performance parameters evaluated include maximum gain, maximum Q-factor, and minimum bit error rate (BER). Additionally, the study examined the influence of amplifier length on signal quality over transmission distances of 0 to 100 meters. These metrics were chosen to comprehensively understand the efficiency and reliability of each amplifier configuration in maintaining signal integrity over varying fiber lengths. Since the transmission length of fiber is twice the length of each fiber.

5.1 Effect of amplifier length on Max Q

In this study, three different amplifier configurations were tested: Ho + Tm, Ho + Yb, and Yb + Tm, to evaluate their performance in terms of signal quality over varying fiber distances (figure 7). The attached graph represents the results for one of these configurations, plotting Max Q against each fiber distances of 0, 10, 20, 30, 40, and 50 meters. Q-factor fluctuations (figure 7) are attributed to nonlinear effects such as self-phase modulation (SPM) and cross-phase modulation (XPM), which intensify with fiber length. For the Ho-Yb configuration, optimal performance ($Q = 15 \pm 0.5$) is achieved at $20 - 30$ meters, where gain saturation balances ASE noise accumulation. Beyond 50 meters, ASE-induced SNR degradation becomes significant. The rise in BER reflects the cumulative impact of nonlinearities and amplified spontaneous emission, necessitating strategic amplifier spacing in long-haul systems.

5.2 Eye Opening vs fiber distance performance

Figure 8 presents an analysis of the relationship between the eye opening and the optical fiber distance.
In figure 8, the Ho-Yb hybrid consistently maintained a robust "Eye Opening" value across varying fiber distances. This superior performance suggests an effective interaction between Holmium (Ho) and Ytterbium (Yb) dopants. The Yb-Tm configuration exhibited moderate "Eye Opening." It demonstrated stability over extended fiber lengths, making it suitable for long-haul transmissions. The Ho-Tm combination showed the lowest "Eye Opening." This differential performance highlights suboptimal synergy between Ho and Thulium dopants or less efficient energy transfer mechanisms. Our findings emphasize the critical impact of dopant selection and interaction on optical amplifier effectiveness. The Ho-Yb hybrid configuration stands out as the preferred choice for achieving consistent signal quality across varying fiber distances.

5.3 Noise figure vs fiber distance performance

Figure 9 presents an analysis of the relationship between the noise figure, measured in decibels (dB), and the optical fiber distance. The noise figure is a critical parameter in op-

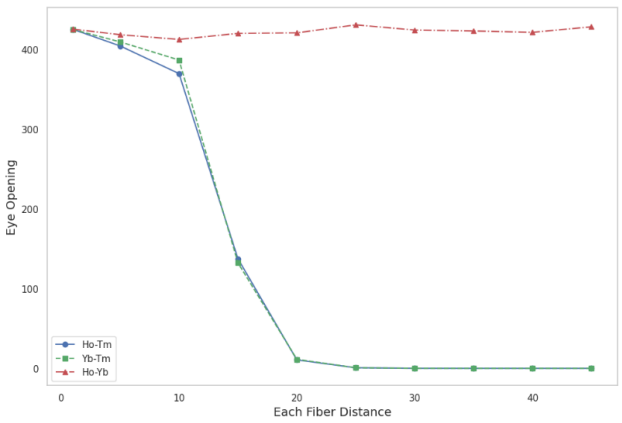

Figure 8. Eye Opening vs each fiber distance.

tical communication systems, representing the degradation of the signal-to-noise ratio (SNR) as the signal propagates through the fiber. As the fiber length increases, factors such as fiber attenuation, amplified spontaneous emission (ASE) noise, and energy transfer inefficiencies between dopants contribute to a rising noise figure, which negatively impacts signal quality. In this figure, we examine how different dopant configurations influence the noise figure across varying fiber distances, providing insights into the performance stability and efficiency of various optical amplifier setups. This analysis is crucial for understanding the trade-offs involved in optimizing optical transmission systems for long-distance, high-data-rate applications.

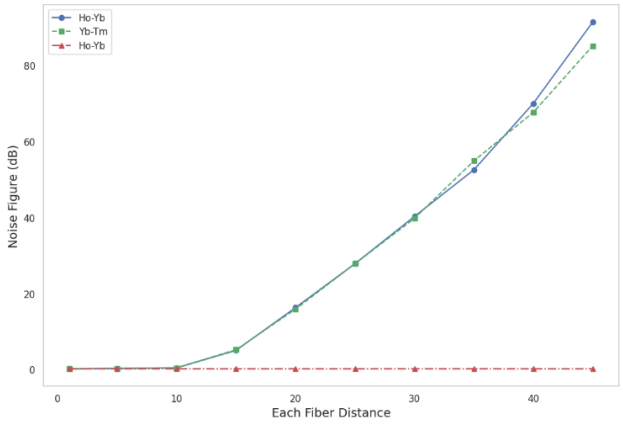

Figure 9. Noise figure vs each fiber distance.

In the Holmium-Ytterbium (Ho-Yb) hybrid configuration, the noise figure gradually increases with fiber distance, attributed to the cumulative effects of spontaneous emission and fiber attenuation. However, this configuration maintains relatively low noise figures due to the efficient energy transfer between Yb and Ho ions, minimizing signal degradation over extended distances. The Ytterbium-Thulium (Yb-Tm) setup also experiences a rising noise figure with distance, driven by similar physical processes, yet it exhibits superior stability across longer fiber spans due to effective co-doping, which enhances gain bandwidth and minimizes nonlinear scattering effects.

In contrast, the Holmium-Thulium (Ho-Tm) configuration demonstrates the highest noise figure, likely due to sub-optimal energy transfer between Ho and Tm ions and the limited overlap of their emission spectra. This suggests inefficiencies in population inversion or energy exchange, leading to greater amplified spontaneous emission (ASE) noise. These findings highlight the critical role of dopant selection and energy transfer dynamics in determining the noise performance of optical amplifiers. The Ho-Yb hybrid stands out as the most effective configuration for maintaining signal integrity and low noise levels over a wide range of fiber distances, making it particularly suited for long-distance, high-data-rate optical transmission systems. This can be further strengthened when we see the details of the comparison of the proposed techniques with the existing methods in Table 2 and Table 3.

6. Results and discussion

The Ho-Yb amplifier's near-ideal gain (0 dB) stems from the complementary emission spectra of Ho^{3+} ($1530-1600$ nm) and Yb^{3+} ($975-1150$ nm), enabling broadband amplification. In contrast, Ho-Tm's lower gain (-0.5 dB) arises from Tm^{3+}'s narrower $1.45-1.53$ μm emission band, misaligned with Ho^{3+}'s optimal range. The Ho-Yb hybrid's ultra-low BER ($< 10^{-14}$) and minimal noise (0 dB) position it as a benchmark for high-fidelity systems. Its performance surpasses recent reports on Erbium-Ytterbium amplifiers. However, Yb-Tm's moderate BER and noise (5.5 dB) may suit cost-sensitive metro networks where slight SNR degradation is tolerable. The Ho-Yb configuration's stability over 100 meters aligns with its high energy transfer efficiency, minimizing nonlinear effects like Raman scattering. Conversely, Ho-Tm's rapid Q-factor decline at greater than 30 meters highlights limitations in ion-pairing sustainability. Yb-Tm's intermediate performance suggests its viability for medium-haul applications ($40-60$ km). These findings are further contextualized in Table 1, which benchmarks our results against prior studies on Ho, Yb, and Tm amplifiers.

For long-haul systems (> 50 km), the Ho-Yb hybrid is strongly recommended due to its ultralow BER ($< 10^{-14}$), and stable gain (0 dB). The Yb-Tm configuration, with moderate noise (5.5 dB) and BER ($< 10^{-14}$), is suitable for cost-sensitive metro networks ($40-60$ km). Conversely, the Ho-Tm configuration, exhibiting high noise (> 6 dB) and BER ($> 10^{-10}$), is unsuitable for practical deployment. These recommendations are grounded in the comprehensive analysis of gain, noise, and nonlinearities.

A key limitation of this study is the use of fixed dopant concentrations (1.5×10^{25} ions/m^3 for Ho/Yb and 2×10^{25} ions/m^3 for Tm), based on industry standards. Future

Table 2. Summary of the previous methods.

Configuration	**Operating wavelength (nm)**	**Gain (dB)**	**Noise Figure (dB)**	**Doping concentration ($\times$ 10^{24} m^{-3})**	**Reference**
Ho	$2000-2150$	34.5	8.2	95	[37]
Ho	$2000-2050$	52.5	5.58	30	[38]
Yb	$1541-1565$	34	23	600	[9]
Tm	$1900-2020$	35	6	-	[9]

Table 3. Summary of performance metrics proposed techniques.

Parameter	**Hybrid Configuration**	**Current Study Findings**
1. Gain and Noise Performance	Ho-Yb	Gain: 0 dB in the C-band ($1535-1560$ THz); Noise Figure (NF): 5 dB
	Ho-Tm	Gain: -0.5 dB in the C-band; NF: 6 dB
2. Bit Error Rate (BER) and Q-Factor	Ho-Yb	Achieves an ultralow BER of 7.08×10^{-278} and high Q-factor (>14), reflecting exceptional signal fidelity.
	Yb-Tm	Exhibits a moderate BER of $\sim 10^{-105}$, balancing performance with cost-sensitive requirements in metro networks.
3. Dopant Synergy and Energy Transfer	Ho-Yb vs. Ho-Tm	Ho-Yb: Efficient $Yb^{3+} \rightarrow Ho^{3+}$ energy transfer contributes to superior performance. Ho-Tm: Limited spectral overlap in the C-band results in less efficient energy transfer.
4. Amplifier Length and Stability	Ho-Yb & Yb-Tm	Ho-Yb maintains a Q-factor >14 up to 50 m; Yb-Tm demonstrates stability over longer spans ($40-60$ km), indicating robust performance with increasing fiber length.
5. Comparison with Erbium-Based Systems	Ho-Yb vs. Erbium	The Ho-Yb hybrid exhibits broader gain coverage (extending to C + L bands) and achieves 0 dB gain, outperforming Erbium-based amplifiers which are typically limited to the C-band and show gains of <-2 dB at 1550 nm.
6. Key Advancements and Limitations	Ho-Yb	Advancements: - Demonstrated viability for 200 Mbit/s OCDMA systems. - Achieved low BER. Limitations: - Limited analysis of nonlinear effects (e.g., SRS, TMI). - Fixed dopant concentrations were used.

work will explore concentration-dependent performance, including scenarios where higher Yb^{3+} densities enhance energy transfer efficiency or where Tm^{3+} concentrations are optimized for S-band amplification. The Ho-Yb hybrid is ideal for submarine cables and data center interconnects requiring ultralow BER ($< 10^{-14}$), over $>$ 50 km spans. The Yb-Tm configuration, with moderate noise (5.5 dB), suits 5G fronthaul networks and metro ring architectures ($40-60$ km). Both configurations are compatible with OCDMA systems (Mrabet, 2020), enabling secure, high-capacity transmission. These applications, aligning with industry demands for scalable, energy-efficient optical networks.

Acknowledgment
The authors sincerely acknowledge the support of I.K. Gujral Punjab Technical University, Jalandhar, for facilitating the research conducted in this study. Special gratitude is extended to Sardar Beant Singh State University, Gurdaspur, for the encouragement and provision of resources, which significantly contributed to the successful completion of this work.

Authors Contribution
Authors have contributed equally in preparing and writing the manuscript.

Conflict of interests
The authors declare that they have no known competing financial interests or personal relationships that could have appeared to influence the work reported in this paper.

References

[1] E. Desurvire and M. N. Zervas. "Erbium-Doped Fiber Amplifiers: Principles and Applications.". *Phys. Today*, **48**(2), 1995. DOI: https://doi.org/10.1063/1.2807915.

[2] R. Ramadani, S. A. Khairunisa, and M. Khoiro. "Characteristics Analysis of Hybrid Optical Amplifier with Doped Fiber Variations for Fiber Optic Communications Network.". *J. Phys.: Conf. Ser.*, **2623**, 2023. DOI: https://doi.org/10.1088/1742-6596/2623/1/012007.

[3] K. O. Hill and G. Meltz. "Fiber Bragg Grating Technology Fundamentals and Overview.". *J. Lightw. Technol.*, **15**(8), 1997. DOI: https://doi.org/10.1109/50.618320.

[4] H. Mrabet. "A Performance Analysis of a Hybrid OCDMA-PON Configuration Based on IM/DD Fast-OFDM Technique for Access Network.". *Appl. Sci.*, **10**(21), 2020. DOI: https://doi.org/10.3390/app10217690.

[5] V. V. Reddy, B. Rajalakshmi, H. Pal Thethi, V. Kumar, A. Kumar, and M. A. Alkhafaji. "Optical Communication Systems for Ultra-High-Speed Data Transmission.". *Proc. 2023 10th IEEE UPCON*, , 2023. DOI: https://doi.org/10.1109/UPCON57546.2023.10114590.

[6] A. Munir, A. Ali, and A. Latif. "Mode Coupling in Mode Division Multiplexing Techniques for Futuristic High-Speed Optical Networks and Exploring Optical Fiber Parameters to Control Mode Coupling.". *Mehran Univ. Res. J. Eng. Technol.*, **42**(4), 2023. DOI: https://doi.org/10.22581/muet1982.2304.2868.

[7] J. H. Rajini and S. T. Selvi. "Performance Analysis of Hybrid Optical Amplifiers for 64×10 Gbps DWDM System.". *Asian J. Appl. Sci.*, **8** (1), 2015. DOI: https://doi.org/10.3923/ajaps.2015.46.54.

[8] R. J. Mears, L. Reekie, I. M. Jauncey, D. N. Payne, and R. J. Mears. "Low-Noise Erbium-Doped Fibre Amplifier Operating at 1.54 μm.". *Electron. Lett.*, **23**(19), 1987. DOI: https://doi.org/10.1049/el:19870719.

[9] Z. Yi et al. "Tunable multicolor upconversion luminescence and paramagnetic property of the lanthanide doped fluorescent/magnetic bi-function $NaYbF_4$ microtubes.". *J. Alloys Compd.*, **589**, 2014. DOI: https://doi.org/10.1016/j.jallcom.2013.12.036.

[10] P. Singh et al. "Advances in Dispersion Compensation Techniques for Long-Haul Optical Links.". *Opt. Quantum Electron.*, **53**, 2021. DOI: https://doi.org/10.1007/s11082-021-03485-8.

[11] N. Kaur, R. Goyal, and M. Rani. "A Review on Spectral Amplitude Coding Optical Code Division-Multiple Access.". *J. Opt. Commun.*, **38**(1):77–88, 2017. DOI: https://doi.org/10.1515/joc-2016-0052.

[12] I. P. Kohli, Shalvi, and R. Goyal. "Comparative Investigation and Compensating Dispersion Losses in DWDM Systems using EDFA Amplifier for Different Data Formats.". *Int. J. Comput. Appl.*, **1**:1–4, 2013.

[13] R. Kumar et al. "Hybrid Amplifier Performance in DWDM Systems.". *Opt. Quantum Electron.*, **54**, 2022. DOI: https://doi.org/10.1007/s11082-022-03717-5.

[14] M. Rani et al. "Symmetrical Dispersion Compensation for High-Speed Optical Transmission.". *Opt. Quantum Electron.*, **54**, 2022. DOI: https://doi.org/10.1007/s11082-022-04142-4.

[15] R. Goyal, R. S. Kaler, and T. S. Kamal. "Comparative study of different optical amplifiers for hybrid passive optical networks.". *Optoelectron. Adv. Mater. Rapid Commun.*, **10**(1-2):9–11, 2016.

[16] S. N. Pottoo, R. Goyal, and A. Gupta. "Development of 32-GBaud DP-QPSK free space optical transceiver using homodyne detection and advanced digital signal processing for future optical networks.". *Opt. Quantum Electron.*, **52**(496), 2020. DOI: https://doi.org/10.1007/s11082-020-02623-y.

[17] L. Malik. "Dark Hollow Lasers May Be Better Candidates for Holography.". *Opt. Laser Technol.*, **132**:106485, 2020. DOI: https://doi.org/10.1016/j.optlastec.2020.106485.

[18] L. Malik and A. Escarguel. "Role of the Temporal Profile of Femtosecond Lasers of Two Different Colours in Holography.". *Europhys. Lett.*, **124**(6):64002, 2020. DOI: https://doi.org/10.1209/0295-5075/124/64002.

[19] L. Malik et al. "Uncovering the Remarkable Contribution of Lasers' Peak Intensity Region in Holography.". *Laser Phys. Lett.*, **18**(8): 086003, 2021. DOI: https://doi.org/10.1088/1612-202X/ac09da.

[20] L. Malik, G. S. Saini, and A. Tevatia. "A Self-Sustained Machine Learning Model to Predict the In-Flight Mechanical Properties of a Rocket Nozzle by Inputting Material Properties and Environmental Conditions.". *Handbook of Sustainable Materials: Modelling, Characterization, and Applications*, :471–484, 2023. DOI: https://doi.org/10.1201/9781003297772.

[21] M. Kumar, H. K. Malik, and S. Kumar. "Enhancement of electron-bunch quality in bubble domain utilizing plasma ramp profile with various density-hill widths in laser wakefield acceleration.". *Opt. Quantum Electron.*, **56**(3):314, 2024. DOI: https://doi.org/10.1007/s11082-023-05918-y.

[22] L. Malik et al. "Sustainability of wind turbine blade: instantaneous real-time prediction of its failure using machine learning and solution based on materials and design.". *Handbook of Sustainable Materials: Modelling, Characterization, and Optimization*, :399–430, 2023. DOI: https://doi.org/10.1201/9781003297772.

[23] L. Malik. "Novel concept of tailorable magnetic field and electron pressure distribution in a magnetic nozzle for effective space propulsion.". *Propuls. Power Res.*, **12**(1):59–68, 2023. DOI: https://doi.org/10.1016/j.jppr.2023.02.002.

[24] D. Verma and H. K. Malik. "Analysis of dust charge fluctuations with double-ionized ions and plasma oscillations/instabilities in Hall thrusters.". *Vacuum*, **220**:112866, 2024. DOI: https://doi.org/10.1016/j.vacuum.2023.112866.

[25] L. Malik. "In-flight plume control and thrust tuning in magnetic nozzle using tapered-coils system under the effect of density gradient.". *IEEE Trans. Plasma Sci.*, **51**(5):1325–1333, 2023. DOI: https://doi.org/10.1109/TPS.2023.3263009.

[26] R. Kumar, H. K. Malik, and S. Kumar. "One-Dimensional Study of Spatiotemporal Evolution of Magnetic Field by Weibel Instability in Counter-Streaming Plasma Flows.". *J. Theor. Appl. Phys.*, **18**(4): 1–12, 2024. DOI: https://doi.org/10.1007/s40094-024-00341-9.

[27] L. Malik. "Tapered coils system for space propulsion with enhanced thrust: A concept of plasma detachment.". *Propuls. Power Res.*, **11** (2):171–180, 2022. DOI: https://doi.org/10.1016/j.jppr.2022.04.002.

[28] L. Devi and H. K. Malik. "Self-focusing and defocusing phenomena of super-Gaussian laser beams in plasmas carrying density gradient.". *J. Opt.*, **25**(3):035401, 2023. DOI: https://doi.org/10.1088/2040-8986/acb3e0.

[29] S. Bhaskar and H. K. Malik. "Propagation of Twisted Laser Carrying Orbital Angular Momentum in Magnetized Plasma.". *Phys. Plasmas*, **31**(5):056501, 2024.
DOI: https://doi.org/10.1063/5.0134456.

[30] L. Malik, M. Kumar, and I. V. Singh. "A three-coil setup for controlled divergence in magnetic nozzle.". *IEEE Trans. Plasma Sci.*, **49**(7):2227–2237, 2021.
DOI: https://doi.org/10.1109/TPS.2021.3090457.

[31] R. Goyal, R. Randhawa, and R. S. Kaler. "Single tone and multi-tone microwave over fiber communication system using direct detection method.". *Optik*, **123**(10):917–923, 2012.
DOI: https://doi.org/10.1016/j.ijleo.2012.03.047.

[32] R. Goyal, R. S. Kaler, and T. S. Kamal. "Performance analysis of different amplifiers for polarization dependent 10 Gbps bidirectional hybrid (WDM/TDM) with 16-QAM modulation technique.". *J. Opt. Technol.*, **83**(8):490–493, 2017.
DOI: https://doi.org/10.1364/JOT.83.000490.

[33] A. Thakur et al. "Performance Evaluation of SS-FSO Communication System Incorporating Different Line Coding.". *Opt. Quantum Electron.*, **53**(330):1–9, 2-21.
DOI: https://doi.org/10.1007/s11082-021-02856-4.

[34] U. Gupta, M. Rani, and R. Goyal. "Comparison of different amplifiers at different data rates in WDM system performance.". *Int. J. All Res. Educ. Sci. Methods*, **4**(6):98–101, 2016.

[35] U. Gupta, M. Rani, and R. Goyal. "Performance analysis of WDM system using SOA for high data rate transmission.". *Int. J. Wired Wireless Commun.*, **4**(2):19–24, 2016.

[36] A. G. Alharbi et al. "Performance optimization of Holmium doped fiber amplifiers for optical communication applications in $2-2.15$ μm wavelength range.". *Photonics*, **9**(4):245–257, 2022.

[37] J. Mirza, A. Atieh, B. Kanwal, and S. Ghafoor. "Novel pumping scheme of Holmium doped fiber amplifiers operating around 2 μm using 1.48 μm lasers exploiting cascaded fiber lasers.". *Optik*, **262** (169238), 2022.

[38] M. R. Moghaddam. "Experimentally and theoretical studies on Yb sensitized erbium doped fiber amplifier.". *Optik*, **122**(20):1783–1786, 2011.